JSR

Journal of Sedimentary Research, 2025, v. 95, 946–958
Research Article
DOI: 10.2110/jsr.2024.153

THE STRATIGRAPHIC RECORD OF THE ARRIVAL OF THE SACRAMENTO AND SAN JOAQUIN RIVERS TO THE CALIFORNIA COAST, U.S.A.

LEAH X. KAHN,[1,2]* YIMING ZHANG,[1†] SETH FINNEGAN,[2] EBEN B. HODGIN,[1,3] AND NICHOLAS L. SWANSON-HYSELL[1†]
[1]*Department of Earth and Planetary Science, University of California, Berkeley, California, U.S.A.*
[2]*Department of Integrative Biology, University of California, Berkeley, California, U.S.A.*
[3]*Department of Earth, Environmental and Planetary Sciences, Brown University, Providence, Rhode Island, U.S.A.*
e-mail: lxkahn@stanford.edu

ABSTRACT: **The Merced Formation is a Pleistocene sedimentary succession of shallow marine and coastal deposits exposed just south of San Francisco, California. Merced Formation strata record a change in sedimentary provenance from local Franciscan Complex sources to detritus from the relatively distant Sierra Nevada batholith. This provenance change is interpreted to represent the establishment of the modern Sacramento–San Joaquin river system, which today drains into the San Francisco Bay estuary. The provenance change was originally identified in a rich unpublished heavy-mineral data set, which we have digitized and reanalyzed using modern statistical approaches. We further confirm this provenance shift with targeted heavy-mineral data developed through quantitative evaluation of minerals by scanning electron microscopy (QEMSCAN). While this provenance shift is striking in heavy-mineral data, it is more subtle in detrital-zircon data due to extensive overlap between zircon age populations of the Franciscan Complex and the Sierra Nevada batholith. New magnetostratigraphic data place constraints on the position of the Brunhes–Matuyama reversal in the succession. Using these magnetostratigraphic data and the 598 ± 13 ka Rockland ash above the provenance shift to develop a Bayesian age model gives an estimate of 633 ka for the age of the provenance shift with a 95% highest density interval between 708 and 608 ka. This timing matches the prediction that the establishment of the Sacramento–San Joaquin river system occurred following the draining of a large paleolake (Lake Clyde) in the California Central Valley, allowing Sierran detritus to reach the California coast.**

INTRODUCTION

The Sacramento and San Joaquin River watersheds together form one of the major river systems in California, draining approximately 40% of the state's land area (Conomos et al. 1985). These rivers converge in the Sacramento–San Joaquin Delta, which discharges into the San Francisco Bay estuary. The Sacramento and San Joaquin rivers define a major north–south axial drainage network through the Central Valley (Fig. 1A). The south-flowing Sacramento River originates in the Klamath Mountains in northern California, while the north-flowing San Joaquin River has its headwaters in the southern Sierra Nevada. Both rivers are fed by major tributaries that drain large areas of the plutonic rocks of the Sierra Nevada batholith, although the Sacramento River drainage area also includes the Klamath Mountains, Lassen Volcanic Center, and western Sierra Nevada Foothills belt (Fig. 1A). The two rivers flow along the north–south axis of the Central Valley and converge at the Sacramento–San Joaquin Delta. From the delta, the river system flows across the Coast Ranges through the Carquinez Strait and into the present-day San Francisco Bay estuary, where it interfaces with the Pacific Ocean (Fig. 1A).

The Central Valley is hypothesized to have formed a closed basin before the establishment of this modern drainage system. With no drainage outlet to the ocean, the valley was filled with a large lake, informally named Lake Clyde after U.S. Geological Survey and University of California, Berkeley geologist Clyde Warhaftig (Fig. 1B) (Sarna-Wojcicki 2021). Lake Clyde (also referred to in the literature as Lake Corcoran; Frink and Kues 1954) is represented in the geologic record by the widespread lacustrine Corcoran Clay member of the Turlock Lake and Tulare formations in the San Joaquin Valley (Fig. 1B) (Frink and Kues 1954). Sarna-Wojcicki (2021) also correlated a diatomaceous clay from a drill core in the southern Sacramento Valley near Zamora, California, with the Corcoran Clay, suggesting that at its greatest extent, Lake Clyde occupied the entire San Joaquin Valley and parts of the Sacramento Valley (Fig. 1B). The end of the lake's lifetime is interpreted to be constrained by ash layers in the Corcoran Clay recorded in drill cores near Wasco, California, in the San Joaquin Valley (Fig. 1B) (Davis et al. 1977; Sarna-Wojcicki 2021). The clay at this locality is approximately 14 m thick and forms the uppermost part of the Corcoran Clay stratigraphy. The Corcoran Clay in the Wasco drill core is bracketed by two well-dated ash beds: the Bishop Tuff ($^{206}Pb/^{238}U$ ID-TIMS zircon age of 767.1 ± 0.9 ka; Crowley et al. 2007) near its base and the Lava Creek B ash bed ($^{40}Ar/^{39}Ar$ sanidine age of 631.3 ± 4.3 ka; Matthews et al. 2015) at its top (Fig. 1B). Thus, the youngest known Lake Clyde deposits are ca. 631 ka, the age of the Lava Creek B ash.

* Present Address: Department of Earth and Planetary Sciences, Stanford University, Stanford, California, U.S.A.
† Present Address: Department of Earth and Environmental Sciences, University of Minnesota, Minneapolis, Minnesota, U.S.A.

Published Online: October 2025
Copyright © 2025, SEPM (Society for Sedimentary Geology) 1527-1404/25/095-946

Downloaded from http://pubs.geoscienceworld.org/sepm/jsedres/article-pdf/95/5/946/7357954/10.2110_jsr.2024.153.pdf
by University of Minnesota user

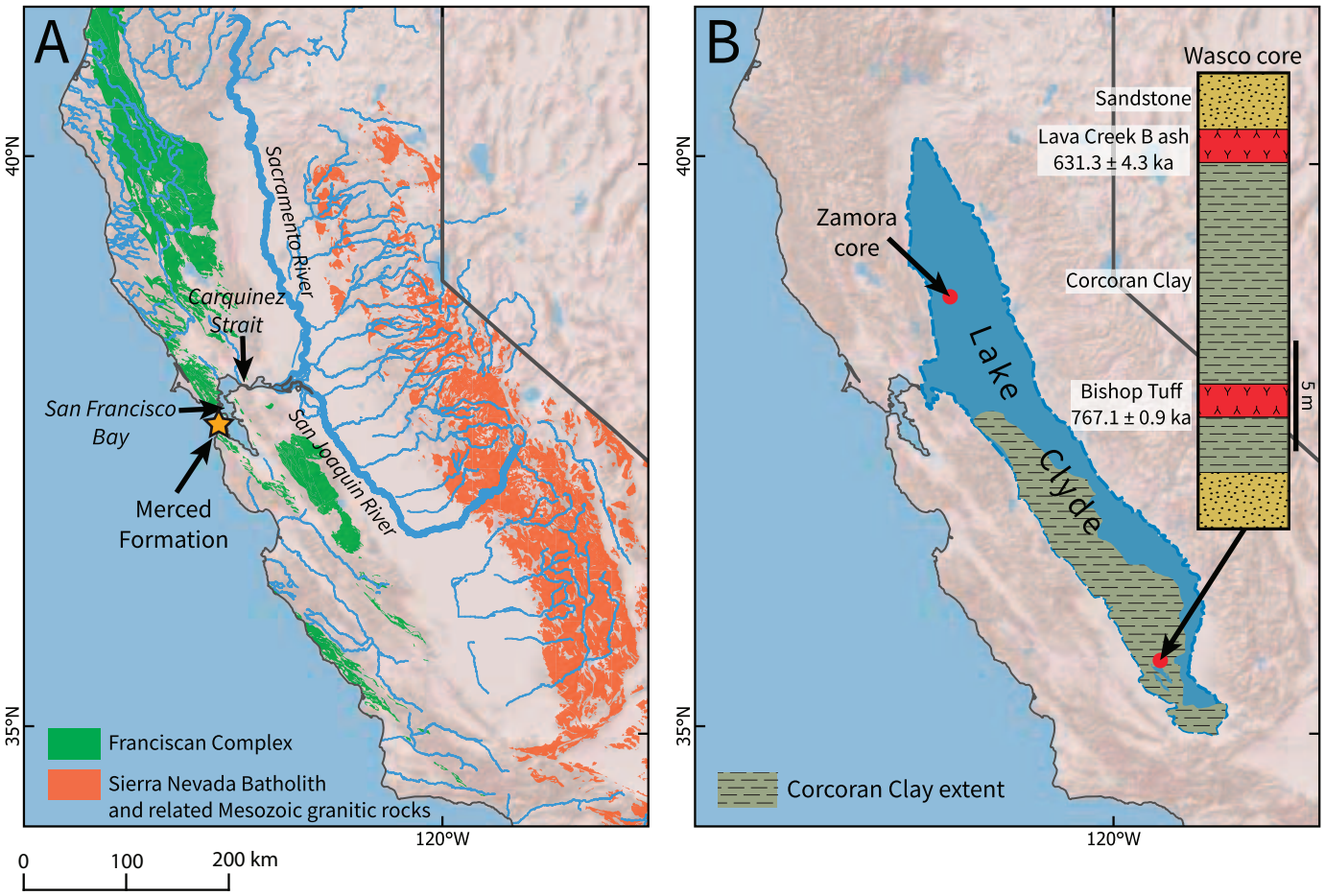

FIG. 1.—**A)** Map of the modern California Central Valley drainage system, with the south-flowing Sacramento River and north-flowing San Joaquin River converging in the San Francisco Bay region. Both rivers drain watersheds in the Sierra Nevada batholith, then flow through the Carquinez Strait to the Pacific Ocean. Bedrock geology is sourced from the USGS State Geologic Map Compilation geodatabase (Horton et al. 2017), and river geometry is sourced from the USGS National Hydrography Dataset (U.S. Geological Survey 2022). **B)** Reconstruction of the maximum extent of Lake Clyde ca. 700 ka, following Sarna-Wojcicki (2021). Extent of the Corcoran Clay follows that used in the USGS Central Valley Hydrologic Model (U.S. Geological Survey 2012). The Wasco core stratigraphy is from Davis et al. (1977) and provides temporal constraints on the duration of Corcoran Clay deposition given the presence of the 767.1 ± 0.9 ka Bishop Tuff (Crowley et al. 2007) and the 631.3 ± 4.3 ka Lava Creek B ash bed (Matthews et al. 2015). Clay in the indicated Zamora core has also been correlated with the Corcoran Clay and associated with Lake Clyde deposition (Sarna-Wojcicki 2021).

Modern Central Valley drainage into the San Francisco Bay region is proposed to have been established following the drainage of Lake Clyde ca. 630 ka (Sarna-Wojcicki 2021). This event is hypothesized to have been a rapid and catastrophic spillover through the Carquinez Strait caused by increased influx of meltwater due to the larger-amplitude climate fluctuations that began at the time of the ca. 700 ka mid-Pleistocene transition (Sarna-Wojcicki 2021). In terms of the current chronology of Pleistocene glaciation (Past Interglacials Working Group of PAGES 2016), an age of ca. 630 ka for the draining of Lake Clyde is consistent with the timing of the glacial-to-interglacial transition associated with marine isotope stage (MIS) 15e (Sarna-Wojcicki 2021).

The major drainage reorganization following the emptying of Lake Clyde had a significant effect on the sediment being delivered to the continental shelf in what is now the San Francisco Bay region. The current estuarine configuration of San Francisco Bay is a recent geomorphologic feature formed during interglacial sea-level rise following a glacial lowstand. At ca. 630 ka, the approximate timing of the draining of Lake Clyde, palinspastic reconstructions along the San Andreas fault place the Point Reyes Peninsula approximately 16 km southeast of its modern position, where it could have formed a topographic barrier at the location of the modern Golden Gate outlet. It is likely that the initial drainage outlet for the Central Valley occupied a location and morphology different from the current estuary, potentially feeding into an embayment that no longer exists (Sarna-Wojcicki 2021). When the drainage first breached through to the coast through the Carquinez Strait, sediment transport is likely to have been more direct to the coast than in the modern-day estuary, where there is sediment accumulation during sea-level highstands (Malkowski et al. 2024).

Before the establishment of the Sacramento–San Joaquin river system, sediment being delivered to the shelf was derived primarily from local Coast Ranges sources, most notably distinctive metamorphic rocks of the Franciscan Complex (Elder 2013). In contrast, sediment delivered by the modern Sacramento–San Joaquin drainage system is mainly derived from the igneous Sierra Nevada batholith (Wong et al. 2013). This change in sedimentary provenance from local Franciscan sources to distant Sierran sources is recorded in the Merced Formation, a succession of Plio(?)-Pleistocene coastal marine and estuarine sediments exposed along the coast south of San Francisco (Fig. 2) (Hall 1965). Following the draining of Lake Clyde, Central Valley drainage to the coast led to increased input of sediment sourced from the Sierra Nevada into the Merced basin (Sarna-Wojcicki 2021). In this study, we seek to evaluate this Merced Formation provenance shift and to test the hypothesis that

Downloaded from http://pubs.geoscienceworld.org/sepm/jsedres/article-pdf/95/5/946/7357954/10.2110_jsr.2024.153.pdf
by University of Minnesota user

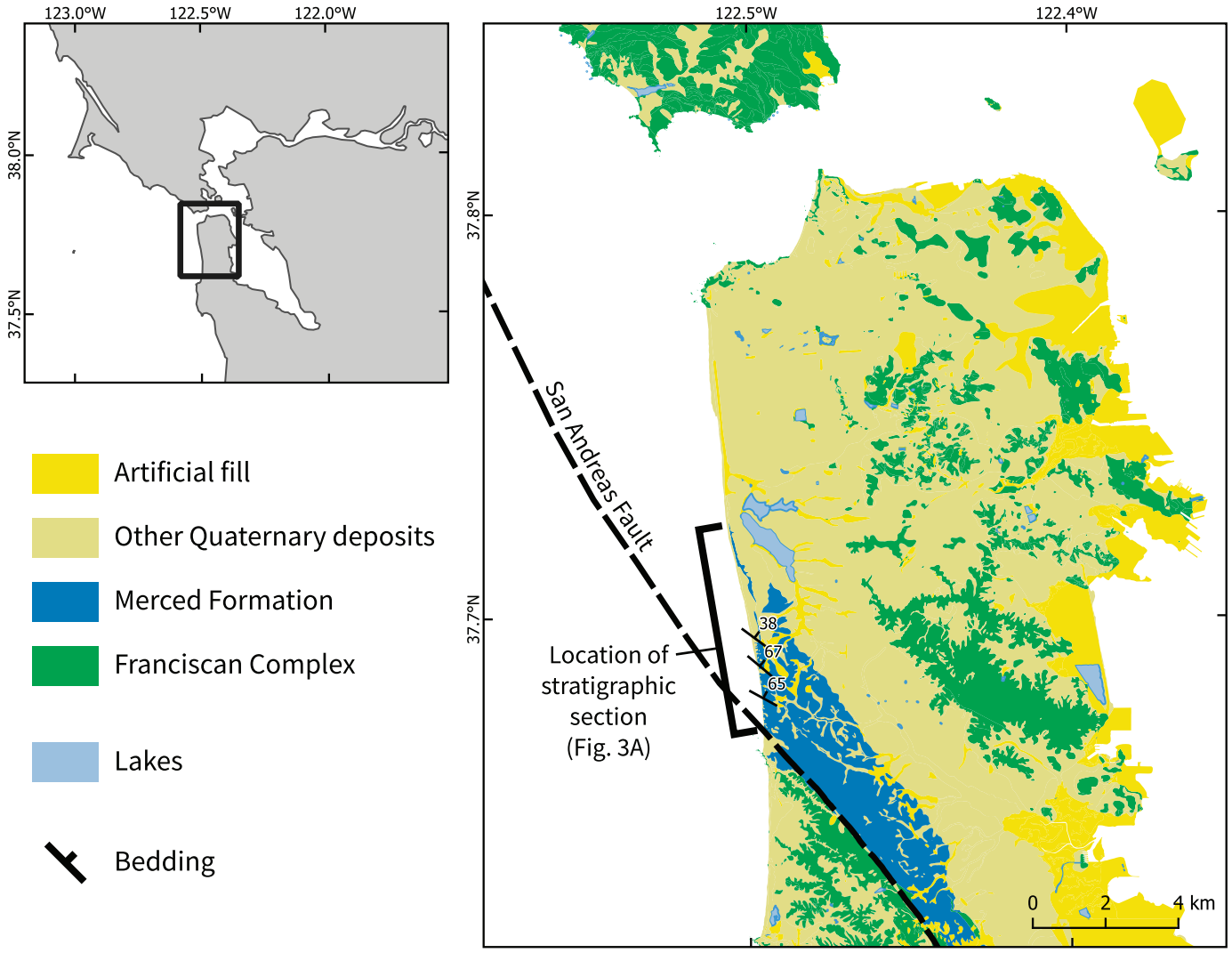

FIG. 2.—Simplified geologic map of the San Francisco Peninsula, with the distribution of the Merced Formation shown in blue. Samples for this study were collected from the stratigraphic section exposed in sea cliffs along the western coast of the peninsula (Fig. 3A). Bedrock geology is sourced from the Digital Geologic Map of Golden Gate National Recreation Area and Vicinity, California (NPS Geological Resources Inventory Program 2009).

the draining of Lake Clyde and the establishment of the Sacramento–San Joaquin drainage system as evidenced by the provenance shift are synchronous.

GEOLOGIC BACKGROUND

Approximately 1,750 m of Merced Formation strata are exposed along coastal cliffs south of San Francisco in a continuous section bounded at its base by the San Francisco Peninsula segment of the San Andreas fault (Figs. 2, 3A). The Merced Formation was deposited in a strike-slip basin which developed along the San Andreas transform fault system. Hengesh and Wakabayashi (1995) proposed that the Merced Formation was deposited in a rapidly subsiding pull-apart basin associated with a localized stepover on the peninsula segment of the San Andreas fault, while Ryan et al. (2008) have argued that the Merced Formation was deposited before initiation of movement on the current fault trace as part of a larger transtensional basin that subsequently became dissected by strike-slip faulting. Postdepositional contractional deformation has uplifted and tilted the Merced strata such that the beds dip consistently to the northeast (Fig. 2; Bruns et al. 2002; Jachens et al. 2002). Dips are generally steep (> 50°) near the base of the section, and become shallower (< 20°) in the upper part of the section farther from the San Andreas fault trace (Clifton and Hunter 1987). The geologically rapid transition from Pleistocene deposition to present-day uplift due to a change from a transtensional to transpressional regime is a hallmark of basins developed through strike-slip faulting (Wakabayashi 2007).

The Merced Formation exhibits an overall shallowing-upward trend, with the lower portion composed mainly of shallow marine shelf deposits, and the upper portion dominated by beach, backshore, and estuarine facies (Fig. 3A). Superimposed on this shallowing-upward trend are variations in lithofacies that have been inferred to reflect changing water depth and thus are interpreted as transgressive–regressive sequences (Clifton 1988; Clifton et al. 1988). Clifton et al. (1988) interpreted at least 30 transgressive–regressive sequences in the Merced Formation, which are proposed to result from eustatic sea-level change accompanying Pleistocene glacial–interglacial cycles. This sedimentologic and stratigraphic framework was extensively developed in a series of publications and field-trip guides (Hunter et al. 1984; Clifton and Hunter 1987; Clifton 1988; Clifton et al. 1988) and has served as the basis for much of the subsequent work on the Merced Formation. $\delta^{18}O$ trends in benthic foraminifera recovered from the section may be consistent with a glacial–interglacial interpretation for the observed facies variability (Green Nylen 2005); however,

Downloaded from http://pubs.geoscienceworld.org/sepm/jsedres/article-pdf/95/5/946/7357954/10.2110_jsr.2024.153.pdf
by University of Minnesota user

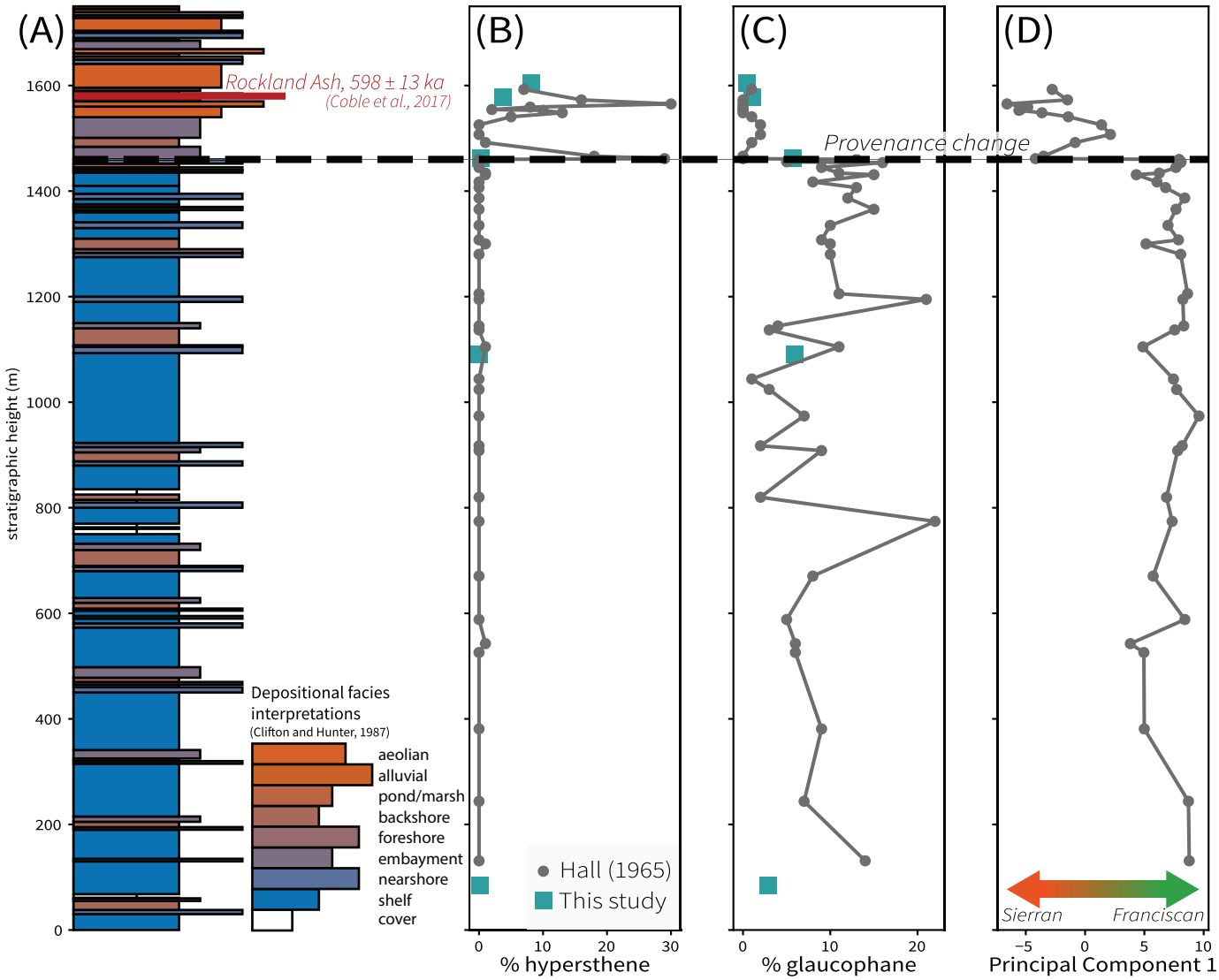

FIG. 3.—Stratigraphy and heavy-mineral-provenance records of the Merced Formation. **A)** The lithostratigraphy is plotted as the interpreted depositional environments of Clifton and Hunter (1987). The lithofacies that are assigned these depositional interpretations are detailed in Table S1. The position of the 598 ± 13 ka Rockland ash is marked by the solid red line (U–Pb zircon date from Coble et al. 2017). **B, C)** The percentages of hypersthene (a mineral representative of Sierra Nevada batholith provenance) and glaucophane (a mineral representative of Franciscan Complex provenance) in heavy-mineral assemblages are shown in stratigraphic position. Gray points are the optical microscopy data of Hall (1965), and blue squares are the QEMSCAN analyses from this study. **D)** Principal component 1 from the principal-component analysis of the heavy-mineral data (Fig. 4) exhibits a sharp shift at the level of the black dashed line indicative of the provenance change.

the data are stratigraphically limited and exhibit high variability which could be associated with alteration.

The change in sedimentary provenance in the Merced Formation from local Franciscan Complex sources to Sierra Nevada batholith and Great Valley Group detritus transported by the Sacramento and San Joaquin rivers occurs 1,460 m above the base of the section (Fig. 3) (Clifton and Hunter 1987). This horizon was first identified by Hall (1965) on the basis of differences in heavy-mineral assemblages of Merced Formation sandstones. Following Hall (1965), we informally divide the Merced Formation into upper and lower members defined by this provenance change. In the lower Merced Formation, there are abundant heavy minerals such as glaucophane and lawsonite that are diagnostic of being sourced from metamorphic rocks of the Franciscan Complex (Fig. 3C). Other metamorphic minerals such as epidote, tremolite–actinolite, and pumpellyite that are consistent with a Franciscan Complex source are also present (Fig. S2). These metamorphic minerals become relatively rare in the upper Merced Formation, where the heavy-mineral assemblage is characterized by abundant hypersthene, hornblende, and augite—likely coming from an igneous protolith and consistent with being sourced from the Sierra Nevada batholith (Figs. 3B, S2). There is also an associated change in feldspar composition, with Na-rich plagioclase (albite) being common in the lower Merced and Ca-rich plagioclase (> An24) becoming more abundant in the upper Merced. This Ca-rich plagioclase is interpreted by Hall (1965) as being derived from an andesitic source. In addition to samples from the Merced Formation, Hall (1965) studied the heavy-mineral composition of modern sands from three potential sediment sources: San Francisco Bay, the Sonoma Volcanics north of the bay, and rivers in the Central Valley. Through comparison with these modern sources, Hall (1965) was able to identify rocks of the Franciscan Complex as the sediment source for the lower Merced Formation and Sierra Nevada detritus delivered via the Sacramento and San Joaquin rivers as the sediment source for the upper Merced Formation. This change in sediment source also corresponds to a transition from marine to terrestrial facies, potentially reflecting progradation

Downloaded from http://pubs.geoscienceworld.org/sepm/jsedres/article-pdf/95/5/946/7357954/10.2110_jsr.2024.153.pdf
by University of Minnesota user

of the shoreline in response to increased sediment flux from the Sacramento–San Joaquin river system (Clifton et al. 1988).

The single well-dated bed in the Merced Formation is an ash bed located approximately 1,580 m above the base of the section (Fig. 3A) (Clifton and Hunter 1987). Petrographic and geochemical analyses of this ash have identified it as a distal deposit of the Rockland ash bed, erupted from the Lassen Volcanic Center in the southern Cascade Range (Sarna-Wojcicki 1976; Sarna-Wojcicki et al. 1985). The Rockland ash is widespread across northern California and Nevada, making it a useful regional chronostratigraphic marker bed (Sarna-Wojcicki et al. 2021). Geochronology studies on the Rockland ash have focused mainly on source-proximal deposits near Lassen Peak. Lanphere et al. (2004) constrained the age of eruption to 610–565 ka based on a combination of $^{40}Ar/^{39}Ar$ dates on plagioclase and U–Pb dates measured on zircon interiors using secondary ion mass spectrometry (SIMS). SIMS U–Pb measurements on crystal faces of zircons from the same locality yield a weighted mean date of 598 ± 13 ka (Coble et al. 2017). This date is in agreement with (U–Th)/He dates from individual zircons, which yield a weighted mean date of 599 ± 12 ka (Coble et al. 2017). The Rockland ash bed in the Merced Formation is located 120 m above the horizon of the provenance change (Fig. 3A), placing a minimum age constraint on the timing of drainage reorganization. Fluvially reworked deposits of the Rockland ash have also been found buried underneath the modern Sacramento–San Joaquin Delta, further suggesting that drainage through the San Francisco Bay region was established by the time of deposition (Maier et al. 2015).

Other than the Rockland ash, there are sparse chronostratigraphic constraints on the Merced Formation. Clifton et al. (1988) described the entire formation as being Pleistocene (younger than 1.6 Ma), based on the occurrence of the echinoid *Scutellaster major* in the lower part of the section. Ingram and Ingle (1998) interpreted an older Pliocene age of 2.4 to 4.3 Ma for the base of the Merced Formation based on measurements of $^{87}Sr/^{86}Sr$ isotopic ratios in fossil benthic foraminifera and mollusks and subsequent comparison to a global seawater strontium reference curve. Their preferred age model indicates a rapid sediment accumulation rate of ~ 1.2 km/Myr above 1,050 m in the section and a rate less than 0.6 km/Myr below that level. However, their data exhibit significant scatter due to the fact that the carbonate fossils measured are preserved in a coarse siliciclastic matrix and therefore poorly protected from alteration given the permeability and lack of carbonate buffering. Alteration in this setting results in lower $^{87}Sr/^{86}Sr$ values due to the sediment being sourced from juvenile Franciscan Complex material with $^{87}Sr/^{86}Sr$ lower than seawater. As seawater $^{87}Sr/^{86}Sr$ has risen through the Pliocene and Pleistocene, alteration to lower $^{87}Sr/^{86}Sr$ values leads to older assigned ages, and therefore this older Pliocene age assignment for the base of the Merced Formation should be viewed with caution.

At its top, the Merced Formation is unconformably overlain by late Pleistocene terrace deposits of the Colma Formation. The 55–75 ka Olema ash bed has been identified in the Colma Formation where it overlies the Merced Formation (Sarna-Wojcicki et al. 1988, 2021; Kuehn and Foit 2006). This ash constrains the age of the Colma Formation and provides a minimum age constraint for the Merced Formation.

If the draining of Lake Clyde was roughly synchronous with the establishment of the Sacramento–San Joaquin drainage network, the end of Lake Clyde deposition can provide a maximum age constraint on the provenance change in the Merced Formation. The presence of the Lava Creek B ash bed (631.3 ± 4.3 ka; Matthews et al. 2015) at the top of the Corcoran Clay suggests that Lake Clyde deposition ended ca. 630 ka (Fig. 1). Given this constraint and the presence of the Rockland ash in the Merced Formation above the provenance change, the timing of the outflow of Lake Clyde and subsequent reorganization of the Central Valley drainage can potentially be constrained to between ca. 600 and ca. 630 ka.

Paleomagnetic data have not been previously published for the Merced Formation but have the potential to provide additional chronostratigraphic constraints. The most recent geomagnetic reversal, the Brunhes–Matuyama reversal, occurred ca. 773 ka (Ogg 2020) and is therefore expected to be recorded in the Merced Formation. The identification of this reversal in the Merced section would provide another absolute age constraint that could be used to infer the timing of drainage reorganization as well as sediment accumulation rates in the Merced Formation.

METHODS

Heavy-Mineral Analysis

In an unpublished UC Berkeley Master's thesis, Hall (1965) developed abundant heavy-mineral data for sand samples using the following approach:

> "The samples were sieved to separate the 60–250 μm size fraction, then split with a microsplitter to provide around 500–1500 grains. The split samples were separated in bromoform (density = 2.89 g/cm^3), and the resulting heavy and light fractions were collected. All heavies from each sample were sprinkled randomly on a slide coated with Canada balsam (refractive index = 1.55) to avoid artificially induced sorting. The heavy minerals were then identified based on optical properties with a petrographic microscope. Minerals were counted using linear traverses across the slide until a total of 100 non-opaque, non-micaceous identifiable grains were recorded for each slide."

Hall (1965) analyzed samples from the Merced Formation, San Francisco Bay, rivers in the Central Valley, and streams draining the Sonoma Volcanics, with the aim of identifying the main sediment sources for the Merced Formation. This dataset comprises 220 samples and over 52,000 individually identified grains, with at least 15 mineral categories identified for each heavy-mineral sample. 85 of the samples and 26,790 of the grains in the dataset come from the section of the Merced Formation covered in this study. Hall (1965)'s discovery in this dataset of a provenance shift from local metamorphic Franciscan sources to igneous Sierran detritus has been referenced in many subsequent publications on the Merced Formation. However, the data themselves have been minimally presented and are available only in two hard copies of the thesis. Here, we digitize these data and make them openly available as Hall et al. (2024). We also reanalyze this rich unpublished data set using modern statistical methods.

We applied principal-component analysis (PCA) to this data set to reduce the dimensionality of the Hall (1965) heavy-mineral data and identify the axes with the greatest variance. As these data are compositional, the constant sum constraint applies (compositions must sum to 100), and the data must be transformed using the centered logratio transform before PCA (Vermeesch 2019). This analysis was done using the robCompositions R package (v. 2.3.1; Templ et al. 2011).

Hall (1965) included modern sediment samples from the Petaluma River, Sonoma Creek, and the Napa River in Napa and Sonoma counties to represent sediment sourced from Neogene Coast Ranges volcanic rocks such as the Sonoma Volcanics. However, preliminary PCA results reveal no overlap between the Sonoma Volcanics samples and the Merced Formation samples, which eliminates the Sonoma Volcanics as a dominant sediment source for the Merced Formation (Fig. S3). Therefore, the Sonoma Creek and Napa River samples were excluded from the PCA to better highlight the distinction between the Franciscan-dominated lower Merced and the Sierra-dominated upper Merced. The Petaluma River samples differ from the Sonoma Creek and Napa River ones in that there are Franciscan Complex rocks in their watershed. These samples were retained in the analysis and reclassified as the "Marin Headlands" sample group (Fig. 4). Although the Marin Headlands samples do have some contribution from Neogene volcanics, they are the best representatives of the Franciscan Complex mineral assemblage in the data set of modern samples. Note that these Petaluma River data are a sparse and geographically limited representation of Franciscan Complex

Downloaded from http://pubs.geoscienceworld.org/sepm/jsedres/article-pdf/95/5/946/7357954/10.2110_jsr.2024.153.pdf
by University of Minnesota user

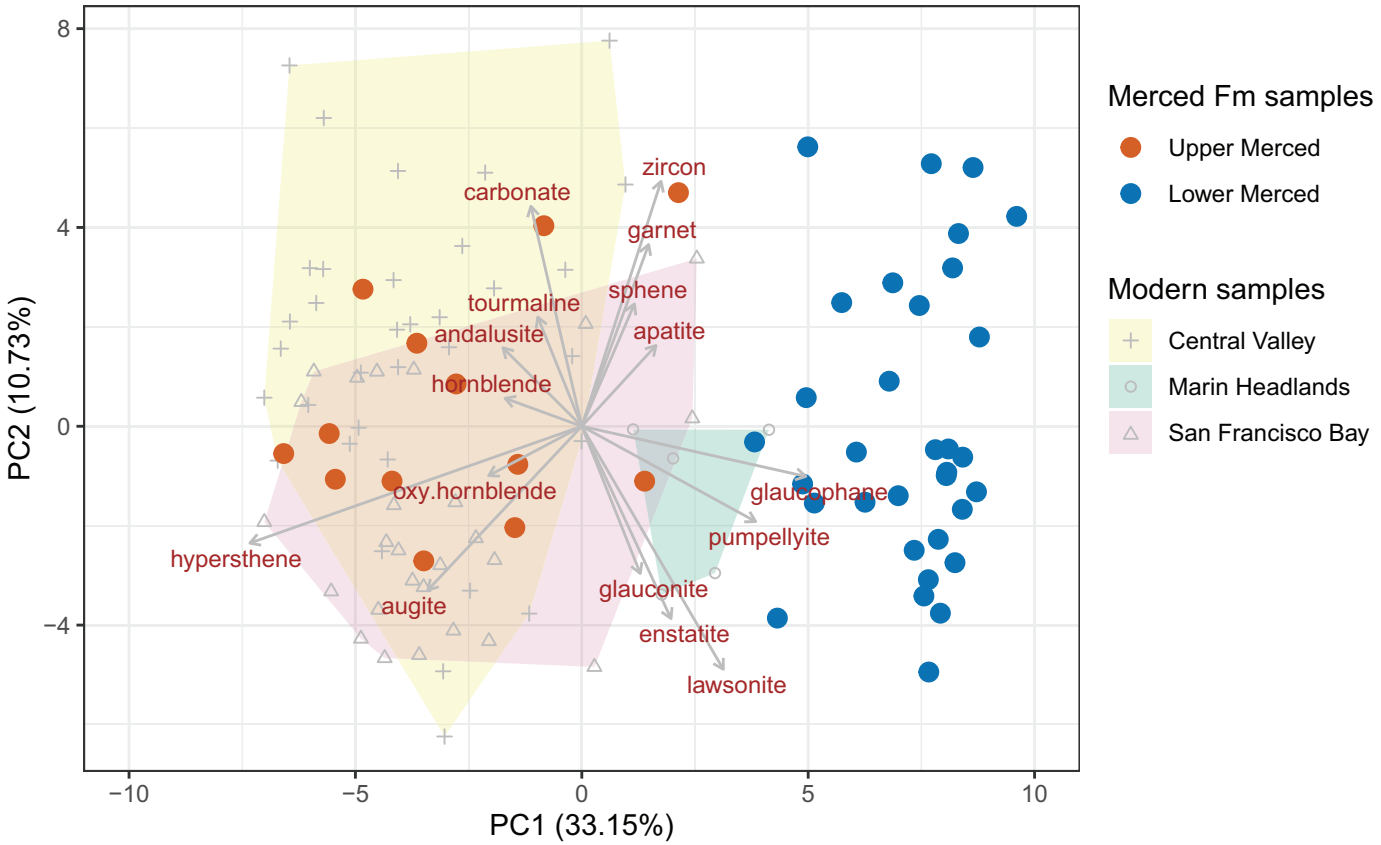

FIG. 4.—Principal-component analysis (PCA) of the heavy-mineral data from Hall (1965) as digitized in Hall et al. (2024). The modern sediment samples are shown as light gray symbols with the areal extent of the data enclosed by colored polygons. The labeled arrows show the loadings for principal components 1 and 2 for the various minerals in the data. There is separation of the upper and lower Merced Formation samples along the first principal component (PC1), with minerals sourced from the Franciscan Complex (e.g., glaucophane) contributing to positive PC1 values and minerals from the Sierra Nevada batholith (e.g., hypersthene) contributing to negative PC1 values. This separation defines the provenance shift labeled in Figures 3 and 5. There is extensive overlap between the upper Merced samples and modern Central Valley and San Francisco Bay sediment samples. The centered log-ratio transformation was applied to the data before analysis using the robCompositions R package (Templ et al. 2011) as is necessary when applying PCA to compositional data.

lithologies relative to the rich data sets from the Central Valley watersheds and San Francisco Bay (Figs. 4, S1).

In addition to reanalyzing the data from Hall (1965), we also generated new heavy-mineral data for five sandstone samples from the Merced Formation collected as part of this study (blue symbols in Figs. 3 and 5). Samples were sieved to isolate the 63–250 μm size fraction, then passed through lithium metatungstate (LMT) heavy liquid with a density of 2.9 g/cm^3 to separate out heavy minerals. Heavy-mineral isolates were then mounted on pucks and analyzed via QEMSCAN (Quantitative Evaluation of Minerals by SCANning electron microscopy) by Rocktype Ltd (Oxford, UK). The QEMSCAN method uses a combination of back-scattered electron signals (BSE) and energy-dispersive X-ray spectra (EDS) collected through scanning electron microscopy to determine a sample's chemical and mineral composition through comparison to known reference materials (Vermeesch et al. 2017). QEMSCAN is advantageous in sedimentary provenance studies because it allows for rapid analysis of high numbers of grains. In this study, the number of grains analyzed in each sample ranges from ~ 8,600 to ~ 56,000 (Fig. S6).

Detrital-Zircon Geochronology

Six samples were collected for detrital-zircon U–Pb analysis (Fig. 5), with the goal of evaluating the Merced Formation provenance change in the zircon populations. Five of these samples (MF22-1, MF22-16, MF22-18, MF22-21, and MF22-22) were also used for QEMSCAN heavy-mineral analysis, while one (MF22-19) did not contain a significant heavy-mineral fraction. Samples MF22-1, MF22-18, and MF22-19 come from below the horizon of the provenance change identified by Hall (1965), sample MF22-16 was collected stratigraphically close to the provenance change, and samples MF22-21 and MF22-22 come from above the change (Fig. 5). MF22-1 (geographic coordinates: 37.6746°, −122.4953°) and MF22-18 (37.6880°, −122.4968°) were collected from relatively uniform beds of medium-grained sandstone below the provenance change that have been interpreted as continental-shelf deposits (Clifton and Hunter 1987). MF22-19 (37.6910°, −122.4975°) is from another medium-grained sandstone bed with a higher proportion of clay-size particles. MF22-16 (37.6941°, −122.4980°) was taken from a 5–10-cm-thick lens of medium-grained sand in a mudstone bed. The samples from above the provenance change of Hall (1965), MF22-21 (37.7153°, −122.5044°) and MF22-22 (37.7191°, −122.5052°), are from beds of medium-grained sandstone immediately below and above the Rockland ash. At all sample locations, the outer weathered surface of the outcrop was scraped away before sample collection in order to avoid contamination from modern beach sand.

Sample MF22-1 was sieved to isolate the < 425 μm size fraction, then hand panned to obtain a heavy fraction. Magnetic separation of the heavies was carried out using a hand magnet and a Frantz magnetic separator. Finally, the nonmagnetic fraction was separated in methylene iodide (density = 3.32 g/cm^3) to isolate zircon grains. Magnetic and heavy-liquid separation techniques were not used for the other samples. Instead, they were only sieved and hand panned, and zircons were picked directly from the heavy fraction

Downloaded from http://pubs.geoscienceworld.org/sepm/jsedres/article-pdf/95/5/946/7357954/10.2110_jsr.2024.153.pdf
by University of Minnesota user

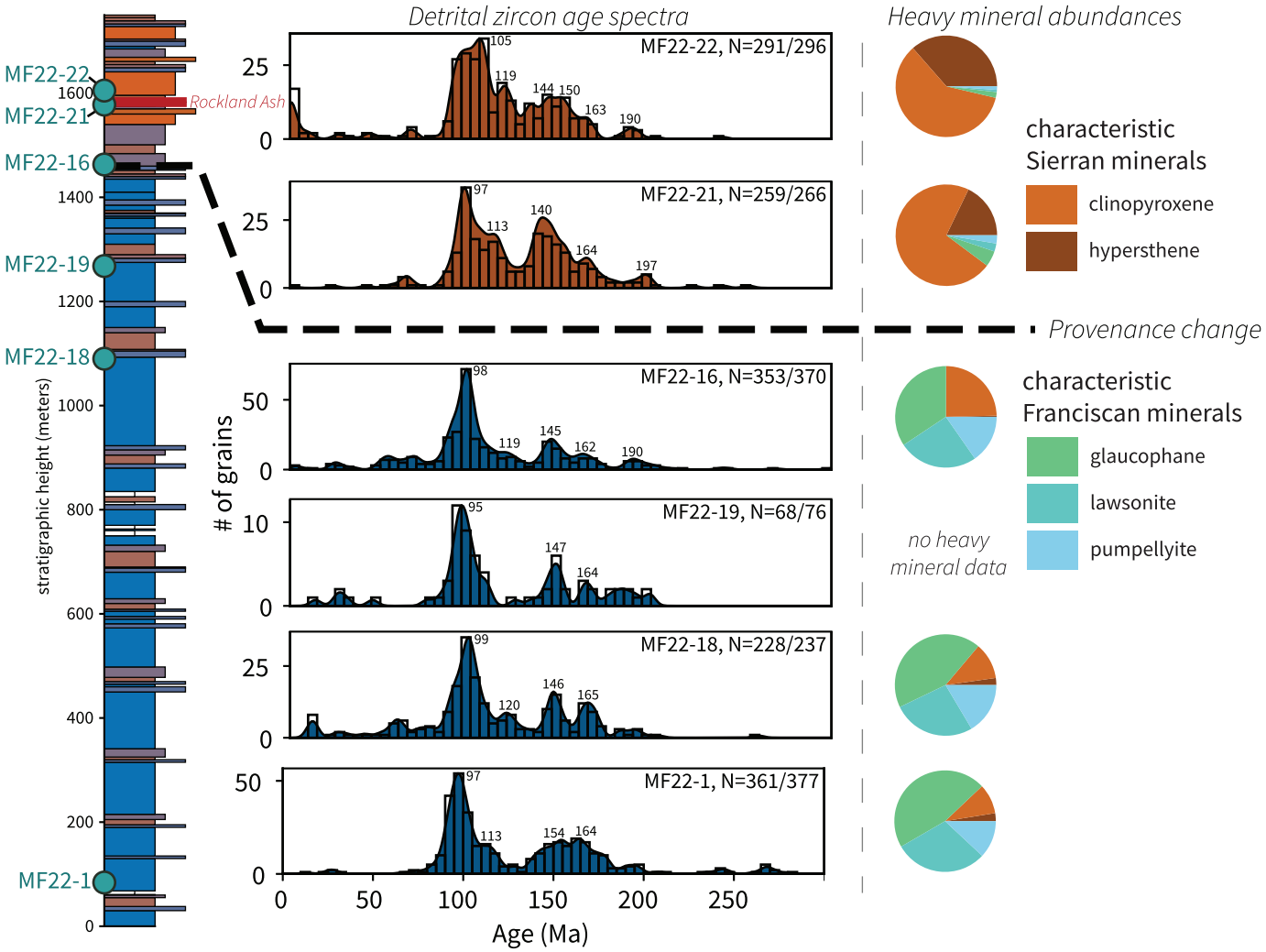

FIG. 5.—Detrital-zircon and heavy-mineral data from the Merced Formation. Sample positions are indicated on the stratigraphic column to the left. The same samples were used for both detrital-zircon and heavy-mineral analyses, with the exception of sample MF22-19, which lacked sufficient heavy minerals for analysis. The detrital-zircon age distributions are shown as histograms with superimposed kernel density estimates (plotted using the detritalPy Python module; Sharman et al. 2018). The blue-shaded spectra represent samples from below the provenance change (indicated with the black dashed line), while the orange-shaded spectra come from above the provenance change. The Merced Formation age distributions are similar below and above the provenance change, and closely resemble the age distributions of potential sources (Fig. S5) (Apen et al. 2021; Bero et al. 2021; Chapman et al. 2012; Prohoroff et al. 2012; Sharman et al. 2015; Snow et al. 2010). The peak in grains younger than 10 Ma in sample MF22-22 likely represents reworked young zircon from the underlying Rockland ash. Pie charts show the abundances of selected source-diagnostic heavy minerals as obtained through QEMSCAN analysis. The mineral abundances have been normalized to the abundance of the five minerals presented in this figure. Below the provenance change, diagnostic Franciscan Complex minerals (glaucophane, lawsonite, and pumpellyite) are abundant, while above the provenance change minerals derived from an igneous source such as the Sierra Nevada batholith (clinopyroxene and hypersthene) dominate.

resulting from hand panning. Hand-picking zircon grains does have the potential to bias grain selection; however, we observed comparable age distributions in sample MF22-1 resulting from both random pour and hand-picking methods (Fig. S4). Approximately 250–400 zircon grains were picked from each sample, with the exception of MF22-19, where 76 grains were picked and analyzed. The zircon grains were mounted in epoxy and polished for imaging and analysis.

The mounted and polished samples were analyzed by LA-ICPMS at the Boise State Isotope Geology Laboratory (MF22-1) following the methods of Hodgin et al. (2022) and the University of California, Santa Barbara, LASS Facility (all other samples) following the methods of Kylander-Clark et al. (2013). Analyses and visualization of detrital-zircon data were done using the detritalPy Python package (v. 1.3.34; Sharman et al. 2018). We visualize the data here as kernel density estimate (KDE) plots (Fig. 5), cumulative density function (CDF) plots (Fig. 6A), and using non-metric multidimensional scaling (NMDS) implemented on Vmax (Fig. 6B). We also show the following intersample comparison metrics computed for probability distribution plots: similarity coefficient, likeness coefficient, Kolmogorov-Smirnov test D value, Kuiper test V value, and cross-correlation coefficient (R^2), following the recommendations of Saylor and Sundell (2016). We used a two-tailed t-test to evaluate the difference between the distribution of these metrics for comparisons within the lower Merced samples and their distribution for comparisons between the lower and upper Merced samples.

Magnetostratigraphy

We collected 2.5-cm-diameter paleomagnetic cores through the Merced strata, starting ~ 5 m above the horizon of the provenance change and continuing downsection (Fig. 7). Samples were collected using a hand-

Downloaded from http://pubs.geoscienceworld.org/sepm/jsedres/article-pdf/95/5/946/7357954/10.2110_jsr.2024.153.pdf
by University of Minnesota user

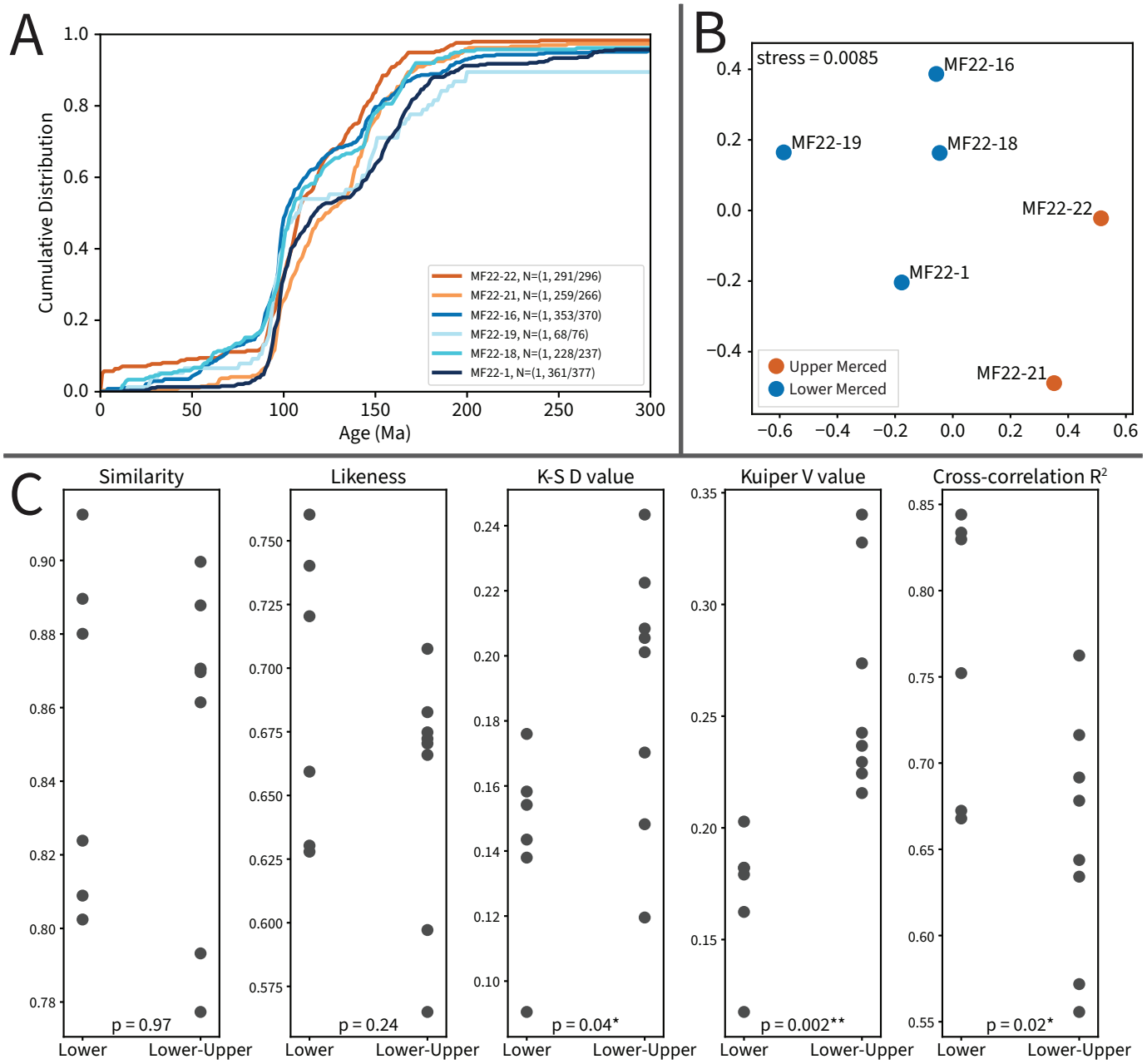

FIG. 6.—Statistical comparison of Merced Formation detrital-zircon samples. **A)** Empirical cumulative distribution functions, calculated at intervals of 1 Myr. **B)** Non-metric multidimensional scaling plot discriminated by Vmax. Final stress value = 0.0085. **C)** Similarity metrics computed for probability-distribution plots. From left to right: similarity coefficient, likeness coefficient, Kolmogorov-Smirnov test D value, Kuiper test V value, and cross-correlation coefficient (R^2). For each subplot, the left column shows values for comparisons within the lower Merced samples. The right column shows values for comparisons between the lower and upper Merced samples. p-values indicate the statistical significance of a two-tailed t-test comparing the distributions. K-S D values ($p = 0.04$), Kuiper V values ($p = 0.002$), and R^2 ($p = 0.02$) are significantly different between lower Merced–lower Merced and lower Merced–upper Merced comparisons, tending toward greater dissimilarity in lower Merced–upper Merced comparisons. These metrics suggest that there is an observable shift in detrital-zircon age distributions between the lower and upper Merced formation, although it is subtle compared to the heavy-mineral signal.

held electric drill and were oriented with a magnetic compass as well as a sun compass when possible. Sun-compass orientations were preferentially used when available. We targeted finer-grained sandstone horizons for sampling because they have lower permeability and are more cohesive. Care was taken to avoid areas where surface weathering had produced visible secondary iron oxyhydroxides.

Samples underwent stepwise alternating-field (AF) demagnetization in the University of California, Berkeley Paleomagnetism Laboratory with peak fields from 1 to 100 mT. Typically, 1 mT steps were used between 1 and 20 mT, 2 mT steps between 20 and 60 mT, and 5 mT steps between 60 and 100 mT. Select samples were also analyzed through stepwise thermal demagnetization. All measurements were made on a 2G DC-SQUID magnetometer equipped with inline AF coils and an automated sample changer system. Least-square fits were made to specimen demagnetization data using the PmagPy software package (Tauxe et al. 2016).

Downloaded from http://pubs.geoscienceworld.org/sepm/jsedres/article-pdf/95/5/946/7357954/10.2110_jsr.2024.153.pdf
by University of Minnesota user

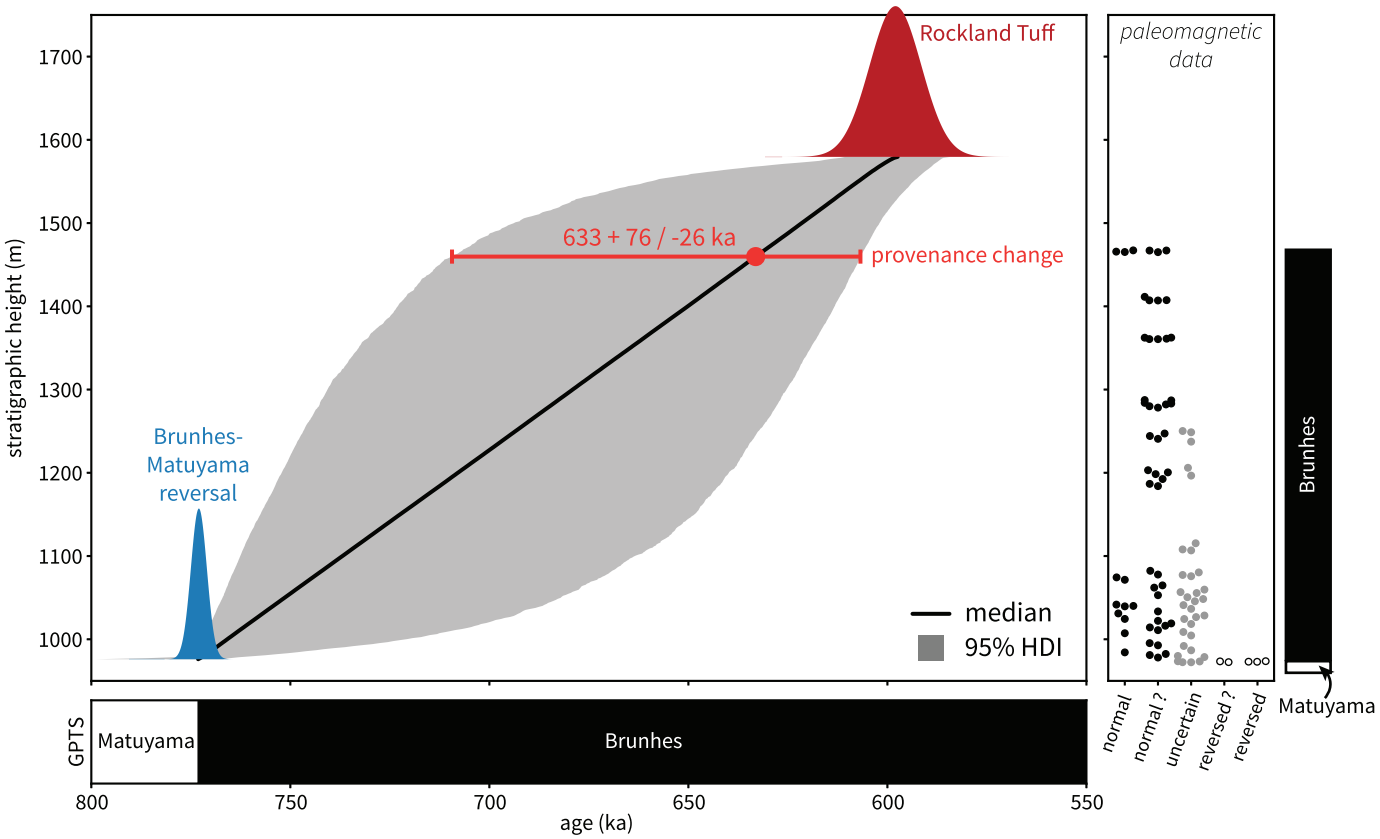

FIG. 7.—A Bayesian age model for the Merced Formation developed using the modified- Bchron R package (https://github.com/robintrayler/modifiedBChron; Trayler et al. 2019). The age constraints used for the model are the 598 ± 13 ka Rockland ash (Coble et al. 2017) at 1580 m in the section and the 773 ± 3 ka Brunhes–Matuyama reversal (Ogg 2020) between 973 and 978 m in the section. The specimen-level interpretations of geomagnetic polarity that lead to this magnetostratigraphic constraint are shown in the right panel with categorizations based on the certainty of the interpretation being: normal, normal?, uncertain, reversed?, and reversed. The probability distributions for both dates are shown with the base of the distributions at their stratigraphic height in the section. In the Bayesian approach, many chronologies are generated through Markov Chain Monte Carlo methods. The 95% highest-density interval (HDI) of these chronologies is shown by the gray region which illustrates the uncertainty between the chronostratigraphic constraints. The age model can be used to estimate the age and associated uncertainty of the provenance change at 1460 m in the section giving an age of 633 ka with a 95% range of 708 to 606 ka.

Bayesian Age–Depth Modeling

We used the existing age constraint from the 598 ± 13 ka Rockland ash (Coble et al. 2017) and new constraints from magnetostratigraphy to develop an age–depth model for the Merced Formation. We applied a Bayesian age–height model framework, because it has the advantage of incorporating uncertainty associated with age constraints and does not impose a linear age model for sediment accumulation. We use the Trayler et al. (2019) implementation of the Bchron model framework of Haslett and Parnell (2008) to develop such a model. Through a Markov Chain Monte Carlo approach, many possible age models are generated, and a highest-density interval (HDI) is defined as the range in the posterior distribution that contains 95% of the age–height paths.

RESULTS

Sedimentary Provenance

Principal-component analysis of data on heavy-mineral abundance from the upper and lower Merced Formation and modern sediments (data from Hall 1965) shows a distinct separation between the upper and lower Merced samples along the first principal component (PC1), which describes approximately 33% of the variance in the data set (Fig. 4). The shift in PC1 values between the upper and lower Merced Formation occurs abruptly in the stratigraphic sequence, suggesting a rapid change in heavy-mineral provenance (Fig. 3D). Higher PC1 values, as seen in the lower Merced Formation samples, are defined by a greater abundance of glaucophane, pumpellyite, and lawsonite—all distinctive minerals of Franciscan Complex metamorphic rocks (Fig. 4). Lower PC1 values, seen in the upper Merced Formation, are defined by abundant hypersthene (an orthopyroxene), augite, and hornblende, which are consistent with the sediment being derived from igneous sources such as the Sierra Nevada batholith (Fig. 4). Modern sediment samples from the Central Valley and San Francisco Bay generally have low PC1 values, while modern sediments from the Petaluma River (which has Franciscan Complex rocks in its watershed) have higher PC1 values (Figs. 4, S1). These modern sediment data provide further support to the interpretation that high PC1 values represent a Franciscan Complex source and low PC1 values represent a Sierra Nevada source. There is extensive overlap between the upper Merced Formation samples and modern San Francisco Bay and Central Valley sediments in PC1 and PC2 space, consistent with the hypothesis that the upper Merced Formation was deposited under the modern Sacramento–San Joaquin River drainage regime (Fig. 4).

QEMSCAN analyses of heavy-mineral samples corroborate the results from Hall (1965), with samples from below the provenance change identified by Hall (1965) having abundant glaucophane, lawsonite, and pumpellyite; and samples from above the provenance change having abundant pyroxenes (Figs. 3, 5, S7). The QEMSCAN results cannot be

Downloaded from http://pubs.geoscienceworld.org/sepm/jsedres/article-pdf/95/5/946/7357954/10.2110_jsr.2024.153.pdf
by University of Minnesota user

directly compared to the Hall (1965) dataset through principal-component analysis due to the difference in methodology and number of mineral types categorized. However, the abundances of source-diagnostic heavy minerals such as glaucophane and hypersthene show similar trends between the two datasets, including a distinct shift at the horizon of the provenance change (Figs. 3, 5, S7).

While there are differences in detrital-zircon age distributions between the upper and lower Merced Formation, they are more subtle than those seen in the heavy minerals (Fig. 5). Such subtlety in differences in zircon age populations is expected due to second-generation recycling of detrital zircon grains from Franciscan Complex sandstones. Overall, the age distributions for our Merced samples largely resemble crystallization ages from the Sierra Nevada batholith, with a large peak around 100 Ma and smaller Late Jurassic peaks between ~ 165 and 145 Ma (Figs. 5, S3) (Chapman et al. 2012). Peaks around 150–145 Ma may also reflect input from Franciscan Complex and/or Great Valley Group sources (Fig. S5) (Snow et al. 2010; Prohoroff et al. 2012; Sharman et al. 2015; Apen et al. 2021; Bero et al. 2021). CDF plots reveal no consistent differences between the upper and lower Merced samples (Fig. 6A). When visualized in multidimensional scaling space, the upper Merced samples do plot near each other, but do not form a clear group separate from the lower Merced samples (Fig. 6B). Similarity and likeness coefficients tend toward being higher within lower Merced samples than when comparing between lower and upper Merced samples, but these differences are not statistically significant. However, cross-correlation coefficients are significantly higher for lower Merced–lower Merced comparisons than for lower Merced–upper Merced comparisons. K-S D values and Kuiper V values also differ significantly between lower Merced–lower Merced and lower Merced–upper Merced comparisons, with within-lower-Merced comparisons having lower values. Taken together, these results do indicate higher similarity within the lower Merced samples than between the upper and lower Merced samples, suggesting that it is possible to distinguish lower Merced and upper Merced samples on the basis of detrital-zircon age data. However, the signal of the provenance shift is more ambiguous in the detrital-zircon data than in the heavy-mineral data.

Magnetostratigraphy

Alternating-field (AF) demagnetization initially removed a low-coercivity component that persisted to steps of ~ 10 mT. The mean direction of this low-coercivity component in geographic coordinates is similar to the local modern dipole direction, and is therefore interpreted as representing a modern-day local field viscous overprint (Fig. S8).

After this viscous overprint was removed, many specimens had unstable magnetization, while others had a variably resolvable mid-coercivity component that typically demagnetized between 20 and 65 mT. Between meter levels 978 and 1467 in the section, this component in stable samples forms a consistent directional population. In geographic coordinates not corrected for bedding tilt, this direction is distinct from the present-day field, including having a steeper inclination. The declination of this component is brought closer to the modern dipole field direction when corrected for bedding tilt (Fig. S8). When tilt-corrected, the direction of the component is shallow relative to the expected dipole field direction. Such a shallow inclination is expected for magnetization acquired by detrital grains during deposition and further shallowed by compaction. These directions are therefore consistent with the mid-coercivity magnetization having been acquired as a detrital remanent magnetization held by (titano)magnetite that experienced inclination shallowing.

These mid-coercivity component directions are of normal polarity in the interval between 978 to 1467 m in the section just above the provenance shift (Fig. 7). Over a one-meter-thick interval at ~ 973 meters in the section, five samples reveal reversed polarity (Fig. 7). These directions are not well resolved due to large normal overprints and variable stability during demagnetization but are consistent with being antipodal to the normal directions isolated in the strata above (Fig. S8). These polarity interpretations place the transition from reversed to normal polarity between 973 and 978 meters in the section which is likely the result of the 773 ± 2 ka Brunhes–Matuyama reversal (Ogg 2020). Below 973 m, almost all samples either exhibit unstable behavior or are completely overprinted by the present local field direction, making interpretations challenging for the lower part of the section.

DISCUSSION

Shift in Sedimentary Provenance

Reanalysis of the extensive unpublished heavy-mineral data set of Hall (1965) using principal-component analysis and analysis of new samples via QEMSCAN both support the hypothesis of a change in provenance in the Merced Formation associated with the establishment of the modern Sacramento–San Joaquin river system (Figs. 3, 5). Merced Formation samples from below the provenance change exhibit a distinct suite of heavy minerals, most notably lawsonite, pumpellyite, glaucophane, and enstatite. These minerals are consistent with a heavy-mineral assemblage derived from metamorphic Franciscan Complex rocks of the California Coast Ranges, which are characterized by abundant glaucophane and enstatite, with less abundant (but still diagnostic) lawsonite and pumpellyite (Yancey and Lee 1972). PCA results show that samples from the upper Merced Formation are distinct from lower Merced Formation samples, but overlap with modern San Francisco Bay and Central Valley sands (Fig. 4). The San Francisco Bay and Central Valley assemblage is characterized by abundant hornblende, augite, and hypersthene derived from the Great Valley Group and the Sierra Nevada batholith (Yancey and Lee 1972). The sediments of the upper Merced Formation record the first appearance of this Sierran heavy-mineral assemblage in the San Francisco Bay area, marking the initiation of Central Valley drainage, which is hypothesized to be associated with the draining of Lake Clyde (Sarna-Wojcicki 2021).

In contrast to the pattern observed in the heavy minerals, only subtle differences are apparent in the detrital-zircon data developed from upper and lower Merced Formation sediments (Figs. 5, 6). These results are in agreement with previous work that was also unable to identify a provenance shift in the Merced Formation based on detrital zircon (Xiao and Grove 2012; Malkowski et al. 2019). Distinguishing between Sierran and Franciscan provenance based on zircon ages alone is challenging because there is extensive overlap between the zircon populations of these two sources. As the zircon present in Franciscan Complex metasedimentary rocks is derived mainly from the Sierra Nevada arc (Ernst et al. 2009; Bero et al. 2021), both the Franciscan Complex and the Sierra Nevada batholith are dominated by Cretaceous-age grains, and zircon age peaks in Franciscan metasediments correlate with peaks of Sierra Nevada batholith crystallization ages (Fig. S5) (Ernst et al. 2009; Chapman et al. 2012; Bero et al. 2021). One difference potentially driving separation between the upper and lower Merced Formation is a greater abundance of pre-Mesozoic zircon grains in the lower Merced samples (Fig. 6). This may reflect subtle changes due to progressive exhumation and unroofing of the Sierra Nevada between deposition of Sierran-derived Franciscan Complex and Coast Ranges sources of the lower Merced Formation and deposition of the directly Sierran-derived upper Merced Formation. For example, the sediment sources for the lower Merced Formation (the Franciscan Complex and Coast Ranges strata) may have a greater proportion of detrital zircon derived from Sierran roof pendants, which are known to be an important source of pre-Sierran grains in Mesozoic strata (Attia et al. 2021).

Studies of modern San Francisco Bay sediments have been able to distinguish sediments sourced from different regions of the Sierra Nevada batholith and those sourced from the California Coast Ranges. The central to southern Sierra Nevada has a higher proportion of middle and Late Cretaceous age grains, while the northern Sierras and Coast Ranges

Downloaded from http://pubs.geoscienceworld.org/sepm/jsedres/article-pdf/95/5/946/7357954/10.2110_jsr.2024.153.pdf
by University of Minnesota user

contain more Jurassic and Early Cretaceous grains (Malkowski et al 2019; Sickmann and Malkowski 2024). Recent work has been able to identify shifting sources of sediment to San Francisco Bay associated with glaciation and deglaciation of the Sierra Nevada in the latest Pleistocene to Holocene (Sickmann and Malkowski 2024) as well as different patterns of sediment supply to subregions of the San Francisco Bay and nearby Pacific coast (Malkowski et al. 2024). These studies required detailed sampling of modern drainages and bay sediments—data which are not available for the drainage and estuary configuration present during deposition of the Merced Formation. The lack of a prominent provenance change in the detrital-zircon data from the Merced Formation suggests complexity in the Merced sediment sources that differs from the arrangement seen in the modern San Francisco Bay, perhaps including greater contributions from Salinian block granitic rocks or from less well-characterized Franciscan Complex and Coast Ranges sources. Further detrital-zircon studies of the Merced Formation along with more specific identification of source rocks has the potential to improve our understanding of sediment transport in the San Francisco Bay region before establishment of the modern bay itself. As it stands, however, it is challenging to apply detrital-zircon geochronology to gain insight into the provenance change in the Merced Formation. In this setting, heavy-mineral analyses provide a clearer picture of changing provenance due to the distinct metamorphic and igneous mineral assemblages found in the Franciscan Complex and Sierra Nevada batholith.

The Age of the Provenance Change

Although the directions are not well resolved, the presence of paleomagnetic samples with reversed polarity at ~ 973 meters in the Merced section indicates a transition from normal to reversed polarity around this stratigraphic interval associated with the Brunhes–Matuyama reversal. With the 598 ± 13 ka age for the Rockland ash above the provenance change and the constraint on the position of the 773 ± 2 ka Brunhes–Matuyama reversal below, an age model can be constructed using a Bayesian age–height model framework to establish an estimate for the timing of the provenance shift (Fig. 7). The gray region in Figure 7 illustrates the resulting highest-density interval (HDI). The age model gives a median age estimate of 633 ka for the stratigraphic level of the provenance shift with a 95% range of 709 to 607 ka (Fig. 7).

Geomagnetic excursions in the Brunhes chron do introduce complexity into the interpretation of the position of the Brunhes–Matuyama reversal in the section. The presence of the 598 ± 13 ka Rockland ash excludes most of these excursions from the section; however, it does not rule out the presence of the ca. 680 ka Osaka Bay excursion (Ogg 2020). While it is possible that the reversed-polarity samples identified in this study result from this Osaka Bay excursion rather than the Brunhes–Matuyama reversal, the uncertainty associated with our estimate for the age of the provenance change is large enough that it encompasses this possibility.

The best estimate for the demise of Lake Clyde in the Central Valley is the 631 ± 4.3 ka age of the Lava Creek B tuff (Matthews et al. 2015), which is at the top of the Corcoran Clay interpreted to have been deposited in the lake (Fig. 1) (Sarna-Wojcicki 2021). Our estimate of 633 ka (with a 95% range of 708–606 ka) for the arrival of Sierra Nevada-derived sediments to the coast overlaps with this timing for the end of Lake Clyde. These chronostratigraphic constraints on the arrival of Sierra Nevada detritus to the Merced Formation are consistent with the hypothesis of Sarna-Wojcicki (2021) that the shift is the result of the establishment of the Sacramento–San Joaquin river system associated with the draining of Lake Clyde.

Sarna-Wojcicki (2021) suggests that Lake Clyde overflowed at the location of the Carquinez Strait (Fig. 1) due to an influx of meltwater during the transition from the glacial interval of marine isotope stage (MIS) 16 to the interglacial recorded by MIS 15. Such an event would be akin to that seen in Lake Bonneville, where the lake level highstand and overflow events are associated with deglaciation following the last glacial maximum (Benson et al. 2011). The Sierra Nevada experienced repeated episodes of glaciation associated with Pleistocene climatic variations starting ca. 2.6 to 2.0 Ma (Gillespie and Zehfuss 2004; Hildreth et al. 2018), and melting of Sierra Nevada glaciers during the MIS 16 to MIS 15 glacial–interglacial transition would have provided meltwater to Lake Clyde. The MIS 16 to MIS 15 transition is also the first major deglaciation following the ca. 700 ka mid-Pleistocene transition to higher-amplitude climate fluctuations (Dean et al. 2015). The cooler and more extended glacial periods associated with the mid-Pleistocene transition likely led to increased ice volume in the Sierra Nevada, which could have exacerbated the effects of deglaciation on lake levels. A global data compilation places the glacial-to-interglacial transition of MIS 15e at ca. 630 to 625 Ma (Past Interglacials Working Group of PAGES 2016), consistent with the interpretation of a post-glacial-maximum spillover of Lake Clyde. Sedimentary records from the Santa Barbara Basin suggest a rapid MIS 16 to MIS 15 transition starting at 631.5 ka on the California margin (Dean et al. 2015). Dean et al. (2015) also report a warm interstadial episode in MIS 16 from 633.6 to 633.4 ka, consistent with the estimate of 633 ka for the provenance change in the Merced Formation.

In addition to increased influx of meltwater, tectonic evolution of the California Coast Ranges is also required to explain the establishment of the Carquinez Strait as the location where the combined Sacramento and San Joaquin rivers pierce through to the coast. The transition from deposition of Merced Formation strata in a strike-slip basin less than 600,000 years ago to uplift of the same strata as coastal cliffs highlights the dynamic spatiotemporal variability of transform-fault systems. In such a tectonic setting, regions of transpression can rapidly transition to transtensional regimes (and vice versa) due to changes in fault geometry such as migrating stepovers (Wakabayashi 2007). The multiple subparallel fault zones of the East Bay fault system, several of which cross the Carquinez Strait or its vicinity, provide a setting conducive to these stepovers. For example, in the past, the Hayward Fault continued west of its current position (Henschel et al. 2024), but now has a major stepover to the east with a releasing bend that connects with the Rodgers Creek fault (Watt et al. 2016). This geometry now results in subsidence in San Pablo Bay (the northern extension of San Francisco Bay; Parsons et al. 2003) which facilitates sediment transport to the coast. Together, rising lake level during glacial retreat and diminished topography at the location of the Carquinez Strait due to fault stepovers could have led to the draining of Lake Clyde. The resulting establishment of a Sacramento–San Joaquin river system draining to the California coast was a formative event in the paleogeographic evolution of California that led to the origin of the present-day San Francisco Bay estuary.

CONCLUSIONS

Reanalysis of the heavy-mineral data set from Hall (1965) quantifies the presence of a shift from a glaucophane/lawsonite/pumpellyite-bearing metamorphic-mineral assemblage to a hypersthene/augite/hornblende-bearing igneous mineral assemblage in the Merced Formation. We reproduce this mineralogical change in new QEMSCAN heavy-mineral analyses. This transition indicates a change in the provenance of Merced Formation sandstones from local Franciscan Complex sources to Sierra Nevada detritus transported by the Sacramento–San Joaquin river system. Additionally, we demonstrate that, despite currently being the most common method used in modern provenance studies, detrital-zircon geochronology is not a straightforward approach for distinguishing the change in provenance in the Merced Formation. The provenance change is likely obscured in such data due to high similarity between zircon populations of the sediment source rocks.

New magnetostratigraphic data allow for the identification of the 773 ± 3 ka Brunhes–Matuyama reversal in the Merced Formation section. We used this

Downloaded from http://pubs.geoscienceworld.org/sepm/jsedres/article-pdf/95/5/946/7357954/10.2110_jsr.2024.153.pdf
by University of Minnesota user

new constraint in combination with the existing constraint from the 598 ± 13 ka Rockland ash (also found in the section) to develop a Bayesian age model for the deposition of the upper part of the Merced Formation. The age model gives an age estimate of 633 ka (95% range of 708–606 ka) for the shift in provenance from Franciscan Complex to Sierra Nevada sources. This age estimate is consistent with the hypothesis of Sarna-Wojcicki (2021) that the provenance change in the Merced Formation is correlated with the draining of paleo–Lake Clyde out of the Central Valley ca. 631 ka and subsequent establishment of the Sacramento–San Joaquin river system. The drainage reorganization following the demise of Lake Clyde was a key event in the development of the present-day California river configuration that delivers freshwater and sediment to the San Francisco Bay estuary.

ACKNOWLEDGMENTS

Project research was supported by the University of California, Berkeley Earth and Planetary Science Department Ramsden Fund for undergraduate research and by the Esper S. Larsen, Jr. Research Fund. Scientific Research and Collecting Permit GOGA-2023-SCI-0008 issued by the National Park Service is gratefully acknowledged. Andrew Kylander-Clark generated LA-ICP-MS data at the University of California, Santa Barbara. Wilma Swanson-Hysell, Ethan Kahn, Diego Afanador Osorio, and Wesley Henschel assisted with fieldwork. We thank Matthew A. Malkowski, Glenn R. Sharman, and Associate Editor Devon A. Orme for reviews that greatly improved the manuscript. Digitized data from Hall (1965) are available as Hall et al. (2024) on Zenodo (https://doi.org/10.5281/zenodo.12347616). Data and code developed for this study are available on Zenodo (https://doi.org/10.5281/zenodo.13352157; Kahn et al. 2024) with paleomagnetic data archived in the MagIC database (https://doi.org/10.7288/V4/MAGIC/20188).

REFERENCES

Apen, F.E., Wakabayashi, J., Day, H.W., Roeske, S.M., Souders, A.K., and Dumitru, T.A., 2021, Regional-scale correlations of accreted units in the Franciscan Complex, California, USA: a record of long-lived, episodic subduction accretion, *in* Wakabayashi, J., and Dilek, Y., eds., Plate Tectonics, Ophiolites, and Societal Significance of Geology: A Celebration of the Career of Eldridge Moores: Geological Society of America, Special Paper 552, p. 233–255, doi:10.1130/2021.2552(11).

Attia, S., Paterson, S.R., Saleeby, J., and Cao, W., 2021, Detrital-zircon provenance and depositional links of Mesozoic Sierra Nevada intra-arc strata: Geosphere, v. 17, p. 1422–1453, doi:10.1130/GES02296.1.

Benson, L.V., Lund, S.P., Smoot, J.P., Rhode, D.E., Spencer, R.J., Verosub, K.L., Louderback, L.A., Johnson, C.A., Rye, R.O., and Negrini, R.M., 2011, The rise and fall of Lake Bonneville between 45 and 10.5 ka: Quaternary International, v. 235, p. 57–69, doi:10.1016/j.quaint.2010.12.014.

Bero, D.A., Anfinson, O.A., and Raymond, L.A., 2021, New insights on Franciscan Complex geology, architecture, depositional age, and provenance for the western Mt. Tamalpais area, Marin County, California: International Geology Review, v. 63, p. 1563–1595, doi:10.1080/00206814.2020.1785338.

Bruns, T.R., Cooper, A.K., Carlson, P.R., and McCulloch, D.S., 2002, Structure of the submerged San Andreas and San Gregorio Fault Zones in the Gulf of the Farallones off San Francisco, California, from high-resolution seismic-reflection data, *in* Parsons, T.E., ed., Crustal Structure of the Coastal and Marine San Francisco Bay Region, California: U.S. Geological Survey, Professional Paper 1658, p. 77–117, doi:10.3133/pp1658.

Chapman, A.D., Saleeby, J.B., Wood, D.J., Piasecki, A., Kidder, S., Ducea, M.N., and Farley, K.A., 2012, Late Cretaceous gravitational collapse of the southern Sierra Nevada batholith, California: Geosphere, v. 8, p. 314–341, doi:10.1130/GES00740.1.

Clifton, H.E., 1988, Sedimentologic approaches to paleobathymetry, with applications to the Merced Formation of Central California: Palaios, v. 3, p. 507–522, doi:10.2307/3514723.

Clifton, H.E., and Hunter, R.E., 1987, The Merced Formation and related beds: a mile-thick succession of late Cenozoic coastal and shelf deposits in the seacliffs of San Francisco, California, *in* Hill, M.L., ed., Decade of North American Geology, Centennial Field Guides: Geological Society of America, Cordilleran Section, v. 1, p. 257–262, doi:10.1130/0-8137-5401-1.257.

Clifton, H.E., Hunter, R.E., and Gardner, J.V., 1988, Analysis of eustatic, tectonic, and sedimentologic influences on transgressive and regressive cycles in the Upper Cenozoic Merced Formation, San Francisco, California, *in* Kleinspehn, K.L., and Paola, C., eds., New Perspectives in Basin Analysis: New York, Springer, Frontiers in Sedimentary Geology, p. 109–128, doi:10.1007/978-1-4612-3788-4_6.

Coble, M.A., Burgess, S.D., and Klemetti, E.W., 2017, New zircon (U-Th)/He and U/Pb eruption age for the Rockland tephra, western USA: Quaternary Science Reviews, v. 172, p. 109–117, doi:10.1016/j.quascirev.2017.08.004.

Conomos, T.J., Smith, R.E., and Gartner, J.W., 1985, Environmental setting of San Francisco Bay: Hydrobiologia, v. 129, p. 1–12, doi:10.1007/BF00048684.

Crowley, J.L., Schoene, B., and Bowring, S.A., 2007, U–Pb dating of zircon in the Bishop Tuff at the millennial scale: Geology, v. 35, p. 1123–1126, doi:10.1130/G24017A.1.

Davis, P., Smith, J., Kukla, G.J., and Opdyke, N.D., 1977, Paleomagnetic study at a nuclear power plant site near Bakersfield, California: Quaternary Research, v. 7, p. 380–397, doi:10.1016/0033-5894(77)90029-1.

Dean, W.E., Kennett, J.P., Behl, R.J., Nicholson, C., and Sorlien, C.C., 2015, Abrupt termination of Marine Isotope Stage 16 (Termination VII) at 631.5 ka in Santa Barbara Basin, California: Paleoceanography, v. 30, p. 1373–1390, doi:10.1002/2014PA002756.

Elder, W.P., 2013, Bedrock geology of the San Francisco Bay Area: a local sediment source for bay and coastal systems: Marine Geology, v. 345, p. 18–30, doi:10.1016/j.margeo.2013.02.006.

Ernst, W.G., Martens, U., and Valencia, V., 2009, U–Pb ages of detrital zircons in Pacheco Pass metagraywackes: Sierran–Klamath source of mid-Cretaceous and Late Cretaceous Franciscan deposition and underplating: Tectonics, v. 28, no. TC6011, doi:10.1029/2008TC002352.

Frink, J.W., and Kues, H.A., 1954, Corcoran Clay: a Pleistocene lacustrine deposit in San Joaquin Valley, California: American Association of Petroleum Geologists, Bulletin, v. 38, p. 2357–2371, doi:10.1306/5CEAE0A0-16BB-11D7-8645000102C1865D.

Gillespie, A.R., and Zehfuss, P.H., 2004, Glaciations of the Sierra Nevada, California, USA, *in* Ehlers, J., and Gibbard, P., eds., Quaternary Glaciations: Extent and Chronology: Elsevier, Developments in Quaternary Sciences, v. 2, p. 51–62, doi:10.1016/S1571-0866(04)80185-4.

Green Nylen, N., 2005, A multi-proxy approach to understanding Plio-Pleistocene climatic and environmental change along the coast of northern California [Ph.D. Thesis]: Stanford University, 295 p.

Hall, N.T., 1965, Petrology of the type Merced group, San Francisco Peninsula, California [M.A. Thesis]: University of California, Berkeley, 127 p.

Hall, N.T., Kahn, L.X., and Swanson-Hysell, N.L., 2024, lxkahn/Hall-1965-data: Digitized data of Hall (1965): Zenodo, doi:10.5281/zenodo.12347617.

Haslett, J., and Parnell, A., 2008, A simple monotone process with application to radiocarbon-dated depth chronologies: Royal Statistical Society, Journal Series C: Applied Statistics, v. 57, p. 399–418, doi:10.1111/j.1467-9876.2008.00623.x.

Hengesh, J.V., and Wakabayashi, J., 1995, Dextral translation and progressive emergence of the Pleistocene Merced basin and implications for timing of initiation of the San Francisco Peninsula segment of the San Andreas Fault, *in* Buising, A.V., Andersen, D.W., and Sangines, E.M., eds., Recent Geologic Studies in the San Francisco Bay Area: SEPM, Pacific Section, p. 47–54.

Henschel, W.G., Hodgin, E.B., Grimsich, J.L., and Swanson-Hysell, N.L., 2024, The Northbrae rhyolite of Berkeley (California, USA) constrains motion of the proto-Hayward Fault: International Geology Review, v. 66, p. 1–15, doi:10.1080/00206814.2024.2355620.

Hildreth, W., Fierstein, J., and Calvert, A.T., 2018, McGee Till: oldest glacial deposit in the Sierra Nevada, California and Quaternary evolution of the rangefront escarpment: Quaternary Science Reviews, v. 198, p. 242–265, doi:10.1016/j.quascirev.2018.08.008.

Hodgin, E.B., Swanson-Hysell, N.L., DeGraff, J.M., Kylander-Clark, A.R., Schmitz, M., Turner, A.C., Zhang, Y., and Stolper, D.A., 2022, Final inversion of the Midcontinent Rift during the Rigolet Phase of the Grenvillian orogeny: Geology, v. 50, p. 547–551, doi:10.1130/G49439.1.

Horton, J.D., San Juan, C.A., and Stoeser, D.B., 2017, The State Geologic Map Compilation (SGMC) Geodatabase of the Conterminous United States: U.S. Geological Survey, Data Series 1052, 46 p., doi:10.3133/ds1052.

Hunter, R.E., Clifton, H.E., Hall, N.T., Császár, G., Richmond, B.M., and Chin, J.L., 1984, Pliocene and Pleistocene coastal and shelf deposits of the Merced Formation and associated beds, northwestern San Francisco Peninsula, California, *in* Hunter, R.E., Clifton, H.E., Hall, N.T., and Chin, J.L., eds., 1984 Midyear Meeting San Jose, California: SEPM, Field Trip Guidebook v. 3, p. 1–29, doi:10.2110/sepmfg.03.001.

Ingram, B.L., and Ingle, J.C., 1998, Strontium isotope ages of the marine Merced Formation, near San Francisco, California: Quaternary Research, v. 50, p. 194–199, doi:10.1006/qres.1998.1990.

Jachens, R.C., Wentworth, C.M., Zoback, M.L., Bruns, T.R., and Roberts, C.W., 2002, Concealed strands of the San Andreas Fault system in the central San Francisco Bay region, as inferred from aeromagnetic anomalies, *in* Parsons, T.E., ed., Crustal Structure of the Coastal and Marine San Francisco Bay Region, California: U.S. Geological Survey, Professional Paper 1658, p. 43–61, doi:10.3133/pp1658.

Kahn, L.X., Zhang, Y., Finnegan, S., Hodgin, E.B., and Swanson-Hysell, N.L., 2024, lxkahn/Merced_Formation_2024: Zenodo, doi:10.5281/zenodo.13352157.

Kuehn, S.C., and Foit, F.F., 2006, Correlation of widespread Holocene and Pleistocene tephra layers from Newberry Volcano, Oregon, USA, using glass compositions and numerical analysis: Quaternary International, v. 148, p. 113–137, doi:10.1016/j.quaint.2005.11.008.

Kylander-Clark, A.R., Hacker, B.R., and Cottle, J.M., 2013, Laser-ablation split-stream ICP petrochronology: Chemical Geology, v. 345, p. 99–112, doi:10.1016/j.chemgeo.2013.02.019.

Downloaded from http://pubs.geoscienceworld.org/sepm/jsedres/article-pdf/95/5/946/7357954/10.2110_jsr.2024.153.pdf
by University of Minnesota user

Lanphere, M.A., Champion, D.E., Clynne, M.A., Lowenstern, J.B., Sarna-Wojcicki, A.M., and Wooden, J.L., 2004, Age of the Rockland tephra, western USA: Quaternary Research, v. 62, p. 94–104, doi:10.1016/j.yqres.2004.03.001.

Maier, K.L., Gatti, E., Wan, E., Ponti, D.J., Pagenkopf, M., Starratt, S.W., Olson, H.A., and Tinsley, J.C., 2015, Quaternary tephrochronology and deposition in the subsurface Sacramento–San Joaquin Delta, California, U.S.A.: Quaternary Research, v. 83, p. 378–393, doi:10.1016/j.yqres.2014.12.007.

Malkowski, M.A., Sharman, G.R., Johnstone, S.A., Grove, M.J., Kimbrough, D.L., and Graham, S.A., 2019, Dilution and propagation of provenance trends in sand and mud: geochemistry and detrital-zircon geochronology of modern sediment from central California (U.S.A.): American Journal of Science, v. 319, p. 846–902, doi:10.2475/10.2019.02.

Malkowski, M.A., Sickmann, Z.T., Fregoso, T., McKee, L., Stockli, D.F., and Jaffe, B., 2024, Reversal in estuarine sand supply driven by Holocene sea level rise: a model for sand transport in large structural estuaries, San Francisco Bay, California, USA: Earth and Planetary Science Letters, v. 643, no. 118887, doi:10.1016/j.epsl.2024.118887.

Matthews, N.E., Vazquez, J.A., and Calvert, A.T., 2015, Age of the Lava Creek supereruption and magma chamber assembly at Yellowstone based on $^{40}Ar/^{39}Ar$ and U–Pb dating of sanidine and zircon crystals: Geochemistry, Geophysics, Geosystems, v. 16, p. 2508–2528, doi:10.1002/2015GC005881.

NPS Geological Resources Inventory Program, 2009, Digital Geologic Map of Golden Gate National Recreation Area and Vicinity, California (NPS, GRD, GRI, GOGA, PORE, MUWO, FOPO, RORI, SAFR, GOGA digital map): National Park Service.

Ogg, J.G., 2020, Geomagnetic polarity time scale, *in* Gradstein, F.M., Ogg, J.G., Schmitz, M.D., and Ogg, G.M., eds., Geologic Time Scale 2020: Elsevier, p. 159–192, doi:10.1016/B978-0-12-824360-2.00005-X.

Parsons, T., Sliter, R., Geist, E.L., Jachens, R.C., Jaffe, B.E., Foxgrover, A., Hart, P.E., and McCarthy, J., 2003, Structure and mechanics of the Hayward–Rodgers Creek fault step-over, San Francisco Bay, California: Seismological Society of America, Bulletin, v. 93, p. 2187–2200, doi:10.1785/0120020228.

Past Interglacials Working Group of PAGES, 2016, Interglacials of the last 800,000 years: Reviews of Geophysics, v. 54, p. 162–219, doi:10.1002/2015rg000482.

Prohoroff, R., Wakabayashi, J., and Dumitru, T.A., 2012, Sandstone matrix olistostrome deposited on intra-subduction complex serpentinite, Franciscan Complex, western Marin County, California: Tectonophysics, v. 568–569, p. 296–305, doi:10.1016/j.tecto.2012.05.018.

Ryan, H.F., Parsons, T., and Sliter, R.W., 2008, Vertical tectonic deformation associated with the San Andreas fault zone offshore of San Francisco, California: Tectonophysics, v. 457, p. 209–223, doi:10.1016/j.tecto.2008.06.011.

Sarna-Wojcicki, A.M., 1976, Correlation of late Cenozoic tuffs in the central Coast Ranges of California by means of trace- and minor-element chemistry: U.S. Geological Survey, Professional Paper 972, p. 1–30, doi:10.3133/pp972.

Sarna-Wojcicki, A.M., 2021, Late Cenozoic paleogeographic reconstruction of the San Francisco Bay area from analysis of stratigraphy, tectonics, and tephrochronology, *in* Sullivan, R., Sloan, D., Unruh, J.R., and Schwartz, D.P., eds., Regional Geology of Mount Diablo, California: Its Tectonic Evolution on the North America Plate Boundary: Geological Society of America, Memoir 217, p. 443–472, doi:10.1130/2021.1217(17).

Sarna-Wojcicki, A.M., Meyer, C.E., Bowman, H.R., Hall, N.T., Russell, P.C., Woodward, M.J., and Slate, J.L., 1985, Correlation of the Rockland ash bed, a 400,000-year-old stratigraphic marker in northern California and western Nevada, and implications for middle Pleistocene paleogeography of central California: Quaternary Research, v. 23, p. 236–257, doi:10.1016/0033-5894(85)90031-6.

Sarna-Wojcicki, A.M., Meyer, C.E., Adam, D.P., and Sims, J.D., 1988, Correlations and age estimates of ash beds in late Quaternary sediments of Clear Lake, California, *in* Sims, J.D., ed., Late Quaternary Climate, Tectonism, and Sedimentation in Clear Lake, Northern California Coast Ranges: Geological Society of America, Special Paper 214, p. 141–150, doi:10.1130/SPE214-p141.

Sarna-Wojcicki, A.M., Sullivan, R., Deino, A., Walkup, L.C., Wagner, J.R., and Wan, E., 2021, Late Cenozoic tephrochronology of the Mount Diablo area within the evolving plate-tectonic boundary zone of northern California, *in* Sullivan, R., Sloan, D., Unruh, J.R., and Schwartz, D.P., eds., Regional Geology of Mount Diablo, California: Its Tectonic Evolution on the North America Plate Boundary: Geological Society of America, Memoir 217, p. 393–441, doi:10.1130/2021.1217(16).

Saylor, J.E., and Sundell, K.E., 2016, Quantifying comparison of large detrital geochronology data sets: Geosphere, v. 12, p., 203–220, doi:10.1130/GES01237.1.

Sharman, G.R., Graham, S.A., Grove, M., Kimbrough, D.L., and Wright, J.E., 2015, Detrital-zircon provenance of the Late Cretaceous–Eocene California forearc: influence of Laramide low-angle subduction on sediment dispersal and paleogeography: Geological Society of America, Bulletin, v. 127, p. 38–60, doi:10.1130/B31065.1.

Sharman, G.R., Sharman, J.P., and Sylvester, Z., 2018, detritalPy: a Python-based toolset for visualizing and analysing detrital geo-thermochronologic data: The Depositional Record, v. 4, p. 202–215, doi:10.1002/dep2.45.

Sickmann, Z.T., and Malkowski, M.A., 2024, A detrital signal of glaciation in the Sierra Nevada, California, U.S.A.: Journal of Sedimentary Research, v. 94, p. 926–936, doi:10.2110/jsr.2024.061.

Snow, C.A., Wakabayashi, J., Ernst, W.G., and Wooden, J.L., 2010, Detrital zircon evidence for progressive underthrusting in Franciscan metagraywackes, west-central California: Geological Society of America, Bulletin, v. 122, p. 282–291, doi:10.1130/B26399.1.

Tauxe, L., Shaar, R., Jonestrask, L., Swanson-Hysell, N.L., Minnett, R., Koppers, A.A.P., Constable, C.G., Jarboe, N., Gaastra, K., and Fairchild, L., 2016, PmagPy: software package for paleomagnetic data analysis and a bridge to the Magnetics Information Consortium (MagIC) Database: Geochemistry, Geophysics, Geosystems, v. 17, p. 2450–2463, doi:10.1002/2016GC006307.

Templ, M., Hron, K., and Filzmoser, P., 2011, Robcompositions: an R-package for robust statistical analysis of compositional data, *in* Pawlowsky-Glahn, V., and Buccianti, A., eds., Compositional Data Analysis: Theory and Applications: John Wiley and Sons, p. 341–355, doi:10.1002/9781119976462.ch25.

Trayler, R.B., Schmitz, M.D., Cuitiño, J.I., Kohn, M.J., Bargo, M.S., Kay, R.F., Strömberg, C.A.E., and Vizcaíno, S.F., 2019, An improved approach to age-modeling in deep time: implications for the Santa Cruz Formation, Argentina: Geological Society of America, Bulletin, v. 132, p. 233–244, doi:10.1130/b35203.1.

U.S. Geological Survey, 2012, Contours of Corcoran Clay thickness in feet by Page (1986) for the Central Valley Hydrologic Model (CVHM): U.S. Geological Survey, Professional Paper 1766, doi:10.5066/P9O6FJ24.

U.S. Geological Survey, 2022, National Hydrography Dataset.

Vermeesch, P., 2019, Exploratory Analysis of provenance data using R and the provenance package: Minerals, v. 9, no. 193, doi:10.3390/min9030193.

Vermeesch, P., Rittner, M., Petrou, E., Omma, J., Mattinson, C., and Garzanti, E., 2017, High throughput petrochronology and sedimentary provenance analysis by automated phase mapping and LAICPMS: Geochemistry, Geophysics, Geosystems, v. 18, p. 4096–4109, doi:10.1002/2017GC007109.

Wakabayashi, J., 2007, Stepovers that migrate with respect to affected deposits: field characteristics and speculation on some details of their evolution, *in* Cunningham, W.D., and Mann, P., eds., Tectonics of Strike-Slip Restraining and Releasing Bends: Geological Society of London, Special Publications, v. 290, p. 169–188, doi:10.1144/SP290.4.

Watt, J., Ponce, D., Parsons, T., and Hart, P., 2016, Missing link between the Hayward and Rodgers Creek faults: Science Advances, v. 2, doi:10.1126/sciadv.1601441.

Wong, F.L., Woodrow, D.L., and McGann, M., 2013, Heavy mineral analysis for assessing the provenance of sandy sediment in the San Francisco Bay Coastal System: Marine Geology, v. 345, p. 170–180, doi:10.1016/j.margeo.2013.05.012.

Xiao, S., and Grove, M., 2012, Detrital zircon evaluation of the provenance shift in the Pleistocene Merced Formation, San Francisco: implications for the timescales of sedimentary processes [Abstract]: American Geophysical Union, Fall Meeting, Abstracts, no. ED31A-0706.

Yancey, T.E., and Lee, J.W., 1972, Major heavy mineral assemblages and heavy mineral provinces of the Central California Coast region: Geological Society of America, Bulletin, v. 83, p. 2099–2104, doi:10.1130/0016-7606(1972)83[2099:MHMAAH]2.0.CO;2.

Received 26 November 2024; accepted 19 August 2025.

Downloaded from http://pubs.geoscienceworld.org/sepm/jsedres/article-pdf/95/5/946/7357954/10.2110_jsr.2024.153.pdf
by University of Minnesota user